doi:10.1093/brain/awaa394 BRAIN 2020: Page 1 of 14 | 1

BRAIN
A JOURNAL OF NEUROLOGY

Modulation of beta bursts in subthalamic sensorimotor circuits predicts improvement in bradykinesia

Yasmine M. Kehnemouyi,[1,†] Kevin B. Wilkins,[1,†] Chioma M. Anidi,[1,2] Ross W. Anderson,[1] Muhammad Furqan Afzal[1,3] and Helen M. Bronte-Stewart[1,4]

[†]These authors contributed equally to this work.

No biomarker of Parkinson's disease exists that allows clinicians to adjust chronic therapy, either medication or deep brain stimulation, with real-time feedback. Consequently, clinicians rely on time-intensive, empirical, and subjective clinical assessments of motor behaviour and adverse events to adjust therapies. Accumulating evidence suggests that hypokinetic aspects of Parkinson's disease and their improvement with therapy are related to pathological neural activity in the beta band (beta oscillopathy) in the subthalamic nucleus. Additionally, effectiveness of deep brain stimulation may depend on modulation of the dorsolateral sensorimotor region of the subthalamic nucleus, which is the primary site of this beta oscillopathy. Despite the feasibility of utilizing this information to provide integrated, biomarker-driven precise deep brain stimulation, these measures have not been brought together in awake freely moving individuals. We sought to directly test whether stimulation-related improvements in bradykinesia were contingent on reduction of beta power and burst durations, and/or the volume of the sensorimotor subthalamic nucleus that was modulated. We recorded synchronized local field potentials and kinematic data in 16 subthalamic nuclei of individuals with Parkinson's disease chronically implanted with neurostimulators during a repetitive wrist-flexion extension task, while administering randomized different intensities of high frequency stimulation. Increased intensities of deep brain stimulation improved movement velocity and were associated with an intensity-dependent reduction in beta power and mean burst duration, measured during movement. The degree of reduction in this beta oscillopathy was associated with the improvement in movement velocity. Moreover, the reduction in beta power and beta burst durations was dependent on the theoretical degree of tissue modulated in the sensorimotor region of the subthalamic nucleus. Finally, the degree of attenuation of both beta power and beta burst durations, together with the degree of overlap of stimulation with the sensorimotor subthalamic nucleus significantly explained the stimulation-related improvement in movement velocity. The above results provide direct evidence that subthalamic nucleus deep brain stimulation-related improvements in bradykinesia are related to the reduction in beta oscillopathy within the sensorimotor region. With the advent of sensing neurostimulators, this beta oscillopathy combined with lead location could be used as a marker for real-time feedback to adjust clinical settings or to drive closed-loop deep brain stimulation in freely moving individuals with Parkinson's disease.

1 Stanford University School of Medicine, Department of Neurology and Neurological Sciences, Stanford, CA, USA
2 The University of Michigan School of Medicine, Ann Arbor, MI, USA
3 Icahn School of Medicine at Mount Sinai, New York, NY, USA
4 Stanford University School of Medicine, Department of Neurosurgery, Stanford, CA, USA

Correspondence to: Helen Bronte-Stewart, MD, MSE
John E. Cahill Family Professor
Director, Stanford Movement Disorders Center (SMDC)
Department of Neurology and Neurological Sciences

Received June 11, 2020. Accepted September 9, 2020.

Rm A343, 300 Pasteur Drive
Stanford University School of Medicine
Stanford, CA 94305, USA
E-mail: hbs@stanford.edu

Keywords: bradykinesia; Parkinson's disease; deep brain stimulation; local field potentials; beta oscillations

Abbreviations: DBS = deep brain stimulation; LFP = local field potential; PSD = power spectral density; rWFE = repetitive wrist-flexion extension; STN = subthalamic nucleus; VTM = volume of tissue modulated

Introduction

It is critical to be able to measure how a biomarker of a given disease changes in response to different doses of any therapy. For example, the efficacy of different doses of anti-hypertensive medications can be easily ascertained by measuring a patient's blood pressure. In contrast, attempts to optimize therapy for Parkinson's disease have consisted of empirical adjustments of doses of medication and/or intensities of deep brain stimulation (DBS) based on a clinical assessment of how such changes affect behaviour and/or produce any adverse effects. No biomarker of the parkinsonian hypokinetic state is available in the chronic clinical setting that is readily accessed and measured in real time to provide critical feedback during adjustments of therapy.

DBS has enabled access to recordings of neural activity [local field potentials (LFPs)] in deep brain structures. Such recordings established that exaggerated neuronal oscillatory activity and synchrony in the beta band (13–30 Hz), known as the beta oscillopathy, may be an electrophysiological biomarker of the hypokinetic state in Parkinson's disease. Beta band power in Parkinson's disease is attenuated in a dose-dependent manner by both high frequency DBS and dopaminergic medication, and the degree of attenuation is related to the improvement in motor behaviour (Brown *et al.*, 2001; Cassidy *et al.*, 2002; Levy *et al.*, 2002; Priori *et al.*, 2004; Wingeier *et al.*, 2006; Kühn *et al.*, 2008; Ray *et al.*, 2008; Bronte-Stewart *et al.*, 2009; Giannicola *et al.*, 2010; Eusebio *et al.*, 2011; Whitmer *et al.*, 2012; Quinn *et al.*, 2015). Beta band oscillatory activity is dynamic and beta burst duration may also be a biomarker of the hypokinetic state in Parkinson's disease. Short ($\leqslant$150 ms) bursts reflect normal sensorimotor processing in non-human primates (Feingold *et al.*, 2015), whereas longer beta burst durations have been correlated with motor disease severity in the resting state, and with gait impairment and freezing of gait (FOG) in Parkinson's disease; improvement in gait and FOG from DBS was associated with a reduction in mean beta band burst durations (Tinkhauser *et al.*, 2017; Anidi *et al.*, 2018; Deffains *et al.*, 2018). This evidence suggests that real-time, simultaneous measures of beta power and beta burst durations while adjusting doses of DBS and medication may be key towards optimizing therapy in Parkinson's disease.

The lack of a clinically available biomarker in Parkinson's disease is further hampered by the fact that DBS efficacy relies on modulation of brain circuitry affected by Parkinson's disease, namely the sensorimotor network, which requires highly accurate placement of the DBS lead in small targets, such as the subthalamic nucleus (STN). Clinical DBS programming has been even less precise because of the lack of clinically approved methods to visualize the anatomic location of the lead once the patient has left the surgical suite. It has been shown that there is a topography of beta power within the STN with higher beta power evident in the dorsolateral sensorimotor portion, which has been theorized to be an effective target for DBS (Vanegas-Arroyave *et al.*, 2016; Horn *et al.*, 2017*a*, *b*; Milosevic *et al.*, 2020). Similarly, investigations into the relationship between lead location and clinical effectiveness of DBS have demonstrated a correlation between modulation of the dorsolateral sensorimotor region and improvement in cardinal motor symptoms of Parkinson's disease (Butson *et al.*, 2011; Dembek *et al.*, 2019).

The combined evidence suggests that more precise STN DBS therapy in Parkinson's disease would be achieved by restoring physiological beta oscillatory activity in the sensorimotor network, using DBS parameters that attenuate beta burst durations and a volume of tissue modulated (VTM) that precisely covers the sensorimotor region in the STN. However, this has not been demonstrated in freely moving individuals with Parkinson's disease, as it has not been possible to simultaneously measure STN beta dynamics and motor behaviour during different intensities of DBS, while demonstrating to what extent VTMs at different intensities encompassed the STN sensorimotor region.

In this study, we demonstrate for the first time the interaction between pathological beta dynamics, the VTM in the STN, and quantitative measures of bradykinesia measured at different intensities of STN DBS. We used the first generation fully implanted sensing neurostimulator (Activa^{TM} PC+S, Medtronic PLC), which made it possible to record synchronized STN neural activity and quantitative kinematic data in freely moving individuals with Parkinson's disease during chronic DBS (Quinn *et al.*, 2015; Trager *et al.*, 2016; Blumenfeld *et al.*, 2017; Syrkin-Nikolau *et al.*, 2017; Anidi *et al.*, 2018; Hell *et al.*, 2018). We posited that with increasing intensities of STN DBS, we would observe (i) progressive improvements in bradykinesia; (ii) a greater reduction in both beta power and beta burst durations during movement; and (iii) a greater overlap of the VTM with the sensorimotor region of the STN. We also hypothesized that the interaction between the amount of tissue modulated in the sensorimotor

STN and the degree of reduction of both beta power and burst durations, would partially explain the improvement in bradykinesia.

Materials and methods

Human subjects

Ten individuals (seven male) with clinically established Parkinson's disease underwent bilateral implantation of DBS leads (model 3389, Medtronic PLC) in the sensorimotor region of the STN using a standard functional frameless stereotactic technique and multi-pass microelectrode recording. Dorsal and ventral borders of each STN were determined using microelectrode recordings, and the base of electrode zero was placed at the ventral border of the STN. The two leads were connected to the implanted investigative neurostimulator [Activa^{TM} PC+S, Medtronic PLC, FDA Investigational Device Exemption (IDE) approved]. The preoperative selection criteria and surgical technique have been previously described (Brontë-Stewart *et al.*, 2010; Quinn *et al.*, 2015). Subjects began experimental testing only after being clinically optimized with chronic DBS settings at the Initial Programming (IP) visit. All experimental testing was done in the OFF medication state, which entailed the withdrawal of long-acting dopamine agonists for 48 h, dopamine agonists and controlled release carbidopa/levodopa for 24 h, and short-acting medication for 12 h prior to the study visit. All participants gave written consent to participate in the study, which was approved by the Food and Drug Administration (FDA) and the Stanford University School of Medicine Institutional Review Board (IRB).

Experimental protocol

Titrations

Recordings were collected in the Stanford Human Motor Control and Neuromodulation Laboratory and were performed OFF dopaminergic medication (withdrawn according to the same timeline as the preoperative protocol). Data were collected at least 60 min after clinical STN DBS was turned off, which we have demonstrated is enough time to wash out the effect of DBS on STN LFPs (Trager *et al.*, 2016). Subjects performed five trials of a seated repetitive wrist flexion-extension (rWFE) task, which we have validated as a measure of bradykinesia in Parkinson's disease (Koop *et al.*, 2006, 2008; Louie *et al.*, 2009; Blumenfeld *et al.*, 2017). Each trial was performed during randomized presentations of STN DBS at 0% (no DBS), 25%, 50%, 75%, and 100% of V_{max}. V_{max} represented the clinically equivalent DBS intensity using a single active electrode, with which neurostimulation improved bradykinesia to a similar degree to that observed when using the clinical DBS intensity delivered through one or multiple electrodes. Subjects were instructed to remain seated and as still as possible with their eyes open during a 60 s rest period, and after a 'Go' command, to flex and extend the hand at the wrist joint as quickly as possible and to stop only when instructed (Fig. 1A); the forearm was flexed so that the elbow was angled at 90°. The movement was self-paced and lasted 30 s. Each subject performed one round of the entire experiment at the designated visit.

Data acquisition and analysis

Local field potential data acquisition

STN LFPs were recorded unilaterally from electrode contact pair 0–2 (13 STNs) or 1–3 (three STNs) on the DBS lead contralateral to the hand moving. LFPs were high-pass filtered at 0.5 Hz, low-pass filtered at 100 Hz, amplified at gains set to minimize stimulation artefact, and sampled at 422 Hz (10-bit resolution). The programmable amplifier embedded in the implanted neurostimulator allowed for setting gains at 250, 500, 1000, and 2000. The gain and centre frequency parameters were chosen for each LFP recording using a standardized protocol that provided a robust method to avoid amplifier overload due to stimulation to record artefact-free signals during stimulation (Blumenfeld *et al.*, 2017). Stimulation for titration experiments (60 μs pulse width, 140 Hz frequency) was delivered through electrode 1 or 2; subject-specific parameters are detailed in Table 1. Uncompressed neural data were recorded on to the Activa^{TM} PC+S system and then extracted via telemetry using the Activa^{TM} PC+S tablet programmer.

Kinematic data acquisition

Movement was measured using solid-state gyroscopic wearable sensors (sampled at 1 kHz) attached to the dorsum of each hand (Motus Bioengineering, Inc) (Fig. 1A) and monitored by continuous video that was synchronized to the kinematic signals.

Angular velocity data were low-pass filtered in MATLAB using two cascaded zero-phase fourth order Butterworth filters with a 4 Hz cut-off frequency. Sampling rates for the angular velocity, accelerometer, and video data were 1 kHz, 1 kHz, and 30 frames per second, respectively.

Synchronization of local field potential and kinematic data

The kinematic and LFP signals were acquired concurrently, using a data acquisition interface (Power1401) and Spike software (version 2.7, Cambridge Electronic Design, Ltd., Cambridge, England). The synchronization of neural and kinematic recordings, using internal and external instrumentation, respectively, was achieved by administering a few seconds of 20 Hz/1.5 V neurostimulation through either DBS lead. The signal artefact was detected concurrently by the implanted system and Spike software, the latter system recording the EEG stimulation artefact using surface electrodes attached to the skin (one on the forehead and one above the implanted neurostimulator), which was recorded at 1 kHz. The files were then co-registered in MATLAB during offline analysis (Quinn *et al.*, 2015).

Data analysis

Spectrograms from LFPs were generated using a short-time Fourier transform of a 1-s sliding Hanning window with 50% overlap. The power spectral density (PSD) estimate was calculated using Welch's method with the aforementioned windows and overlap parameters. PSDs of movement state LFPs (during 30 s of rWFE) were calculated at each stimulation condition. Grand average PSDs were also calculated by averaging movement state LFPs across all STNs at each stimulation condition. To calculate beta power for each STN, the peak frequency in the beta band (13–30 Hz), which was also the frequency at which the PSD power differential between 0% and 100% stimulation was largest, was identified. A 6 Hz band, defined as the

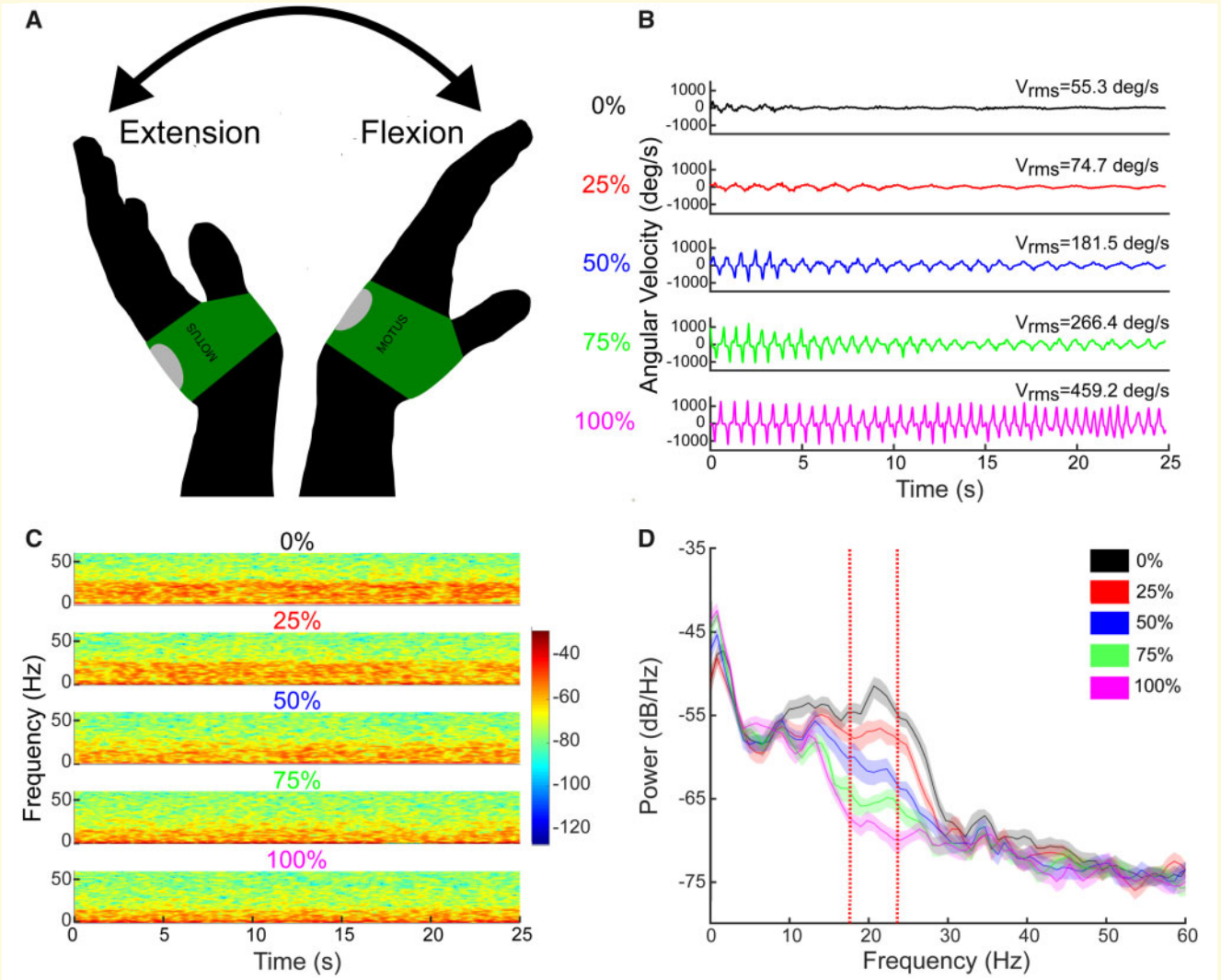

Figure 1 Example of the effect of stimulation on behaviour and beta power. (**A**) Illustration of the repetitive wrist flexion-extension (rWFE) task with the Motus gyroscope attached to the dorsum of the hand. (**B**) Example of angular velocity traces during the rWFE task at each stimulation condition from a representative individual. (**C**) Spectrogram of STN LFPs during the rWFE task at each stimulation condition. The colour bar represents the power in dB/Hz. (**D**) PSD diagrams averaged across the rWFE for each stimulation condition. Vertical red lines identify the 6 Hz beta band of interest. Shading represents 95% confidence intervals.

movement band, was then created and centred on this peak frequency. Relative beta power in the movement band was normalized by dividing these values by the mean power across the 45–65 Hz band during the movement state, enabling comparison among STNs (Syrkin-Nikolau *et al.*, 2017). Grand average box plots were also created for analysis by averaging normalized beta power in each STN's specific movement band at each DBS intensity.

Beta band dynamics

Fluctuations in beta band power over time were measured using a physiological baseline, that captures a broad distribution of fluctuations, characterized as bursts using a method described previously (Anderson *et al.*, 2020). To calculate beta bursts, the raw LFP was filtered with a zero-phase eighth order Butterworth bandpass filter with a 6 Hz bandwidth centred around the movement band frequency described above. The bandpass filtered signal was squared and an amplitude envelope of the maximum power was created by linearly connecting consecutive peaks of the squared LFP signal. The baseline for thresholding was established by filtering the LFP between five overlapping 6 Hz bands in the low gamma band (45–65 Hz), an inert, low power band in the Parkinson spectra that was absent of peaks, and subsequently squaring and creating five power envelopes. The median of the troughs (minima) were calculated from each envelope and averaged. The baseline threshold for bursts was established as four times the median power of the troughs in order to reliably detect gamma power above the estimated device floor of the Activa™ PC+S neurostimulator while still being low enough to reflect the desire for a baseline (Anidi *et al.*, 2018; Anderson *et al.*, 2020). Burst durations were calculated as the interval between successive crossings of the movement band envelope over the baseline. Burst durations were calculated for each STN at 0%, 25%, 50%, 75%, and

Table 1 STN titration parameters

Subject	STN	Active electrode Pulse width = 60 μs Frequency = 140 Hz	V_{max} (V)	Centre frequency (Hz)
1	L	2^-	1.5	23.90
1	R	1^-	3.9	22.25
2	R	1^-	3.6	18.13
3	L	1^-	3.0	19.78
3	R	1^-	2.5	20.61
4	L	1^-	3.0	20.61
4	R	1^-	3.7	22.25
5	R	1^-	4.0	18.96
6	L	1^-	3.5	20.61
7	L	1^-	4.3	19.78
7	R	2^-	4.8	18.96
8	L	1^-	2.5	19.78
9	L	2^-	2.5	28.02
9	R	1^-	3.9	16.48
10	L	1^-	3.0	28.85
10	R	1^-	3.2	23.08

100% V_{max} DBS. The mean burst duration was calculated as the mean of all bursts at each stimulation condition. The degree of reduction of burst duration during DBS was calculated from the per cent change between the mean burst duration at 0% (no DBS) and mean burst duration at 25%, 50%, 75%, and 100% V_{max} DBS, respectively, for each STN.

Kinematic data analysis

Root mean square velocity (V_{rms}) was calculated and logarithmically transformed for each movement epoch to conform to normality. V_{rms} at each stimulation intensity was normalized to the subject's maximum V_{rms} observed among all stimulation conditions in order to compare the effect of stimulation on V_{rms} among subjects. The degree of improvement was calculated as the per cent change between V_{rms} at 0% stimulation and V_{rms} at each of 25%, 50%, 75%, and 100% V_{max} DBS for each STN. Synchronized angular velocity data from the rWFE recordings and neural data from the LFP recordings were segmented using Spike software and analysed using MATLAB (version 9.6, The MathWorks Inc. Natick, MA, USA).

Localization of DBS leads

Preoperative T_1 and T_2 MRI scans and postoperative CT scans were acquired as part of the standard Stanford clinical protocol (Brontë-Stewart *et al.*, 2010). Location of DBS leads was determined by the Lead-DBS toolbox (Horn *et al.*, 2019). Postoperative CT scans and preoperative T_2 scans were co-registered to preoperative T_1 scans, which were then normalized into MNI space using SPM12 (Statistical Parametric Mapping 12; Wellcome Trust Centre for Neuroimaging, UCL, London, UK) and Advanced Normalization Tools (Avants *et al.*, 2011). DBS electrode localizations were then corrected for brain-shift in the postoperative CT scan (Horn and Kühn, 2015). DBS electrodes were then localized in template space using the PaCER algorithm (Husch *et al.*, 2018) and projected onto the DISTAL Atlas to visualize overlap with the STN (Ewert *et al.*, 2018).

Calculation of volume of tissue modulated

VTMs were modelled using the approach described by Horn *et al.* (2019). Electric fields were estimated using a finite element method model with a four-compartment tetrahedral mesh segmenting grey matter, white matter, electrode contacts, and insulating materials. The per cent volume of overlap was then computed for both the whole STN and the sensorimotor portion of the STN based on the DISTAL Atlas (Ewert *et al.*, 2018).

Statistical analysis

Statistics were computed using R (version 3.6.0, R Foundation for Statistical Computing, University of Auckland, New Zealand) and MATLAB. Kolmogorov-Smirnov tests and theoretical-sample quantile plots were used to assess the normality of the distributions of beta power in the movement band, mean beta burst durations, and normalized V_{rms} at each separate stimulation condition (0%, 25%, 50%, 75%, 100% V_{max} DBS), as well as to check for normality of the differences between pairwise comparisons of DBS intensities (0–25%, 0–50%, 0–75%, and 0–100% V_{max} DBS) for each of the above variables. Based on these results, repeated measures ANOVAs followed by Mauchly's test for sphericity were used to compare both mean movement band power and mean beta burst durations across all STN's at the five stimulation conditions. Paired *t*-tests were used *post hoc* to compare the difference in beta power and mean beta burst durations between the 0–25%, 0–50%, 0–75%, and 0–100% V_{max} DBS conditions. Because of its non-normal distribution, a Friedman's test for non-parametric one-way ANOVA compared normalized V_{rms} across all STN's at the five stimulation conditions. Wilcoxon signed-rank tests were used *post hoc* to compare the difference in V_{rms} between the 0–25%, 0–50%, 0–75%, and 0–100% V_{max} DBS conditions. *P*-values for *post hoc* tests were corrected for multiple comparisons using false discovery rate. Linear mixed effects regression models were computed to calculate the association between per cent change in beta burst duration and power on the per cent change in V_{rms}, separately. Per cent change in V_{rms} was included as the dependent variable and per cent change in either beta burst duration or beta power was used as a fixed effect with subject as a random effect to account for within-subject relationships. A similar linear mixed effects regression model was computed with per cent change in either beta burst duration or beta power as the dependent variable and per cent activation of the whole STN or the sensorimotor region of the STN as fixed effects with subject as a random effect. Finally, a linear mixed effects model was computed with per cent change in V_{rms} as the dependent variable and the interaction between per cent change in beta burst duration and the per cent activation of the sensorimotor region of the STN as fixed effects with subject as a random effect.

Data availability

Data will be made available on request when possible.

Results

Sixteen STNs from 10 well-characterized individuals with Parkinson's disease were included in the analysis. The LFPs

Table 2 Subject demographics

Subject	Sex	Age at visit	Years since diagnosis	Pre-op UPDRS (OFF meds)	Pre-op UPDRS (ON meds)	UPDRS at visit (off therapy)	UPDRS at visit(on therapy)
1[b]	Male	56.1	8.2	24	8	35	7
2[a]	Male	65.7	6.2	35	26	25	12
3[b]	Male	68.7	8.2	29	16	20	3
4[b]	Male	60.9	6.1	39	23	48	8
5[a]	Male	45.0	7.3	58	12	56	6
6[a]	Male	56.1	10.2	52	29	55	14
7[b]	Male	36.2	4.0	59	22	63	28
8[a]	Female	52.5	11.1	50	26	43	18
9[b]	Female	53.8	14.2	34	6	15	6
10[b]	Female	58.4	13.2	38	18	36	5
Average ± SD		55.3 ± 9.5	8.9 ± 3.3	41.8 ± 12.2	18.6 ± 8.0	39.6 ± 16.2	10.7 ± 7.6

[a]One STN used.
[b]Both STNs used.

from four STNs were excluded because of a lack of discernible signal: in three STNs this was due to artefact in the beta band during stimulation, and in the other STN this was due to an elevated noise floor. The mean age of the participants was 55.3 ± 9.0 years, and mean disease duration was 8.9 ± 3.1 years. Preoperative OFF and ON medication United Parkinson's Disease Rating Scale (UPDRS) III scores were 41.8 ± 11.6 and 18.6 ± 7.6, respectively. OFF medication UPDRS III scores, off and on STN DBS were 39.6 ± 14.6 and 10.7 ± 7.2, respectively, at the time of the experiment (Table 2). The visit was conducted 2.5 ± 0.6 years after the participant's initial programming visit.

Stimulation improved bradykinesia, reduced beta power and shortened beta burst durations

Figure 1 displays synchronized kinematic and neural data when one individual with Parkinson's disease performed the rWFE task during the randomized presentations of STN DBS at 0%, 25%, 50%, 75%, and 100% of V_{max}.

At increasing DBS intensities, this individual exhibited progressive increases in angular velocity and frequency during rWFE (Fig. 1B), and progressive attenuation of this individual's movement band power (Fig. 1C and D).

Across the group, increasing intensities of STN DBS during rWFE were associated with increases in V_{rms} and attenuation of movement band power (Fig. 2). Figure 2A shows the grand average boxplot of V_{rms} during rWFE, at each intensity of DBS, normalized to the maximum V_{rms} observed for each hand. There was a significant effect of stimulation on V_{rms}, which increased as DBS intensity increased [$\chi^2(15) = 25.05$; $P = 0.049$]. *Post hoc* Wilcoxon signed-rank tests showed significant increases between V_{rms} at baseline and during the 50%, 75%, and 100% V_{max} stimulation conditions: 0% and 50% V_{max} ($Z = 3.10$; $P = 0.0038$), 0% and 75% V_{max} ($Z = 2.90$; $P = 0.0051$), 0% and 100% V_{max} ($Z = 3.52$; $P = 0.0018$). There was no increase in V_{rms} at 25% V_{max} DBS intensity ($Z = 0.98$; $P = 0.33$). Figure 2B demonstrates the grand average PSDs across all STNs at each intensity of DBS, during movement, and Fig. 2C shows the corresponding grand average boxplot for the power in the movement band. The STN-specific movement band was calculated using a 6 Hz band centred on the peak beta band frequency, which was also the beta frequency that was most modulated by DBS during movement; nearly all centre frequencies lied between low and high beta (18–23 Hz) (Table 1). There was a significant effect of stimulation on movement band power: increasing stimulation intensity reduced beta power [$F(4,60) = 6.96$; $P = 0.016$]. *Post hoc* paired *t*-tests showed significant reductions between movement band power at baseline and DBS intensity at all intensities, 0% and 25% [$t(15) = 2.17$; $P = 0.047$], 0% and 50% [$t(15) = 2.44$; $P = 0.037$], 0% and 75% [$t(15) = 2.67$; $P = 0.035$], 0% and 100% [$t(15) = 2.77$; $P = 0.035$].

Decreased beta power and burst durations during DBS titrations correlated with improved bradykinesia

Reduction in movement band burst durations was associated with increases in V_{rms} (Fig. 3). Figure 3A shows the band-pass filtered LFP in the 6 Hz movement band from an individual with Parkinson's disease during rWFE, and Fig. 3B shows the envelope of the squared filtered signal and method for identifying bursts.

There was a significant effect of DBS intensity on movement band burst durations: higher DBS intensities were associated with shorter burst durations (Fig. 3C) [$F(4,60) = 7.75$; $P = 0.011$]. *Post hoc* paired *t*-tests showed significant reductions in burst durations during DBS at 50%, 75%, and 100% V_{max} compared to no DBS (0% V_{max}): 0% and 50% [$t(15) = 2.52$; $P = 0.031$], 0% and 75% [$t(15) = 2.70$; $P = 0.031$], 0% and 100% [$t(15) = 2.99$; $P = 0.031$]. There was a trend between reduction in burst durations during DBS at 25% V_{max} compared to no DBS [$t(15) = 2.07$; $P = 0.056$]. Mean movement band burst durations were

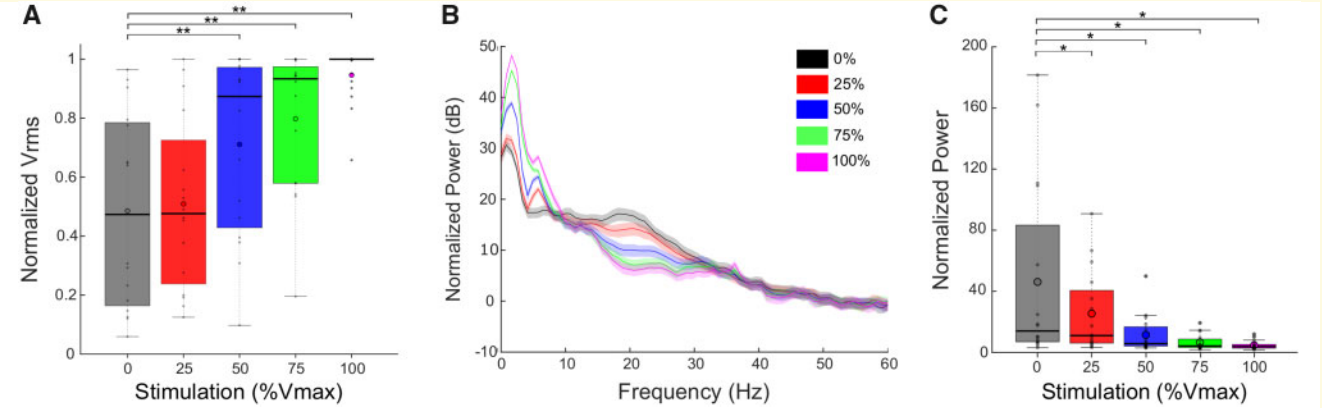

Figure 2 DBS improved behaviour and attenuated beta power. (**A**) Box plots with individual data overlaid depict the V_{rms} during rWFE normalized to the maximum V_{rms} observed for each STN. DBS improved V_{rms}, with significant differences from no stimulation occurring at 50%, 75%, and 100% V_{max}. (**B**) Grand average PSDs for all STNs during rWFE at each DBS intensity. (**C**) Grand average box plots with individual data overlaid depicting averaged normalized power in the movement band of each STN during rWFE at each DBS intensity. Stimulation progressively reduced movement band power, with significant differences from no stimulation occurring at all intensities of DBS. Thick horizontal line represents the median and the open circle represents the mean. *$P < 0.05$, **$P < 0.01$.

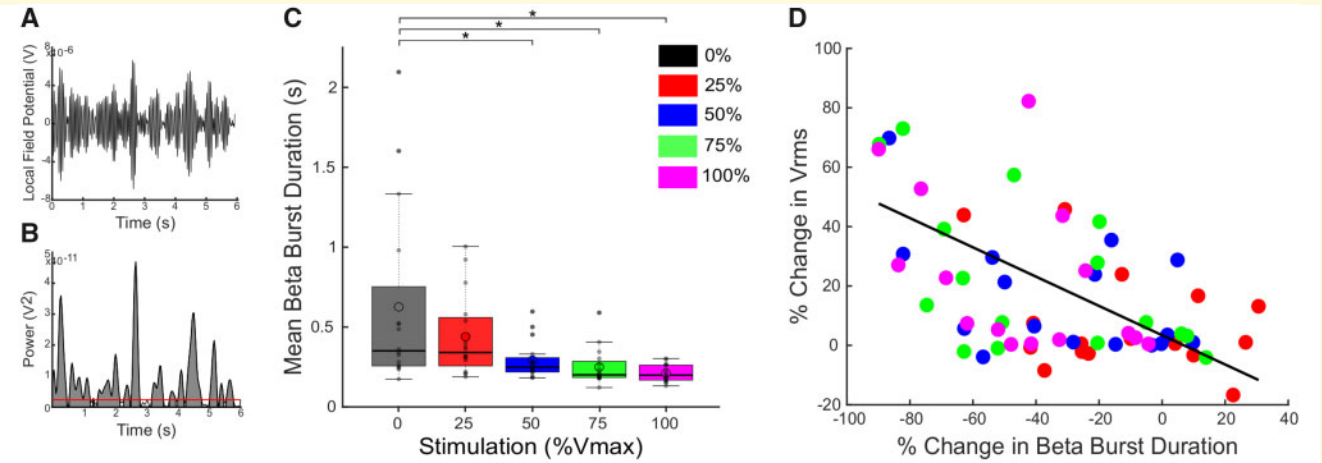

Figure 3 DBS reduced movement band burst durations during rWFE and shorter burst durations were associated with improvement in bradykinesia. (**A**) Bandpass filtered LFP in the 6 Hz movement band during a portion of the rWFE task. (**B**) Envelope of the squared movement band filtered signal in **A**. The red horizontal line denotes the baseline used for burst identification. Shaded grey regions represent identified bursts. (**C**) Box plots with individual data overlaid depicting the movement band burst durations for each stimulation intensity. DBS progressively reduced movement band mean burst duration, with significant differences occurring at 50%, 75%, and 100% V_{max}. (**D**) There was a significant correlation between the % change in movement band burst duration and % change in V_{rms} as calculated by the linear mixed model ($P < 0.001$). Thick horizontal line represents the median and the open circle represents the mean. *$P < 0.05$.

reduced from 626 ± 554 ms off DBS to 439 ± 249 ms at 25% V_{max}, 293 ± 117 ms at 50% V_{max}, 250 ± 112 ms at 75% V_{max}, and 210 ± 5 ms at 100% V_{max}. This trend is also demonstrated in all burst durations across all STNs (Supplementary Fig. 1). As stimulation intensity increased, burst durations were shortened, with longer bursts >1000 ms significantly reduced and mean burst duration of all bursts progressively decreasing from no DBS to 100% V_{max}.

A linear mixed effects regression model was used to assess the relationship between the change in V_{rms} and change in movement band burst durations: decreases in movement band burst durations were associated with increases in V_{rms} ($\beta = -0.53$, $t = 4.50$, $P < 0.001$) (Fig. 3D). A linear mixed effects regression model was also used to assess the relationship between change in V_{rms} and movement band power, from which decreases in movement band power were also associated with increases in V_{rms} ($\beta = -0.48$, $t = 4.19$,

Table 3 Linear mixed models summary

Dependent variable	Predictor	B (95%CI)	β (95%CI)	t-value	P-value
% Change in V_{rms}	% Change in beta burst duration	−0.49 (−0.71 to −0.27)	−0.53 (−0.77 to −0.30)	4.50	3.02×10^{-5}
% Change in V_{rms}	% Change in beta power	−0.37 (−0.54 to −0.19)	−0.48 (−0.70 to −0.25)	4.19	9.07×10^{-5}
% Change in beta burst duration	% STN modulation	−1.00 (−1.25 to −0.75)	−0.42 (−0.53 to −0.32)	7.92	5.40×10^{-11}
% Change in beta burst duration	% sensorimotor STN modulation	−0.51 (−0.61 to −0.41)	−0.47 (−0.56 to −0.38)	10.35	3.87×10^{-15}
% Change in beta power	% STN modulation	−1.24 (−1.60 to −0.88)	−0.43 (−0.56 to −0.31)	6.93	2.87×10^{-9}
% Change in beta power	% sensorimotor STN modulation	−0.65 (−0.79 to −0.50)	−0.49 (−0.60 to −0.38)	9.08	5.33×10^{-13}
% Change in V_{rms}	(% Change in beta burst duration) × (% sensorimotor STN modulation)	−0.00547 (−0.01 to −0.00048)	−0.18 (−0.33 to −0.015)	2.19	0.032
% Change in V_{rms}	(% Change in beta power) × (% sensorimotor STN modulation)	−0.00637 (−0.011 to −0.0017)	−0.25 (−0.43 to −0.066)	2.72	0.0084

B = unstandardized beta coefficient; β = standardized beta coefficient.

$P < 0.001$, data not shown). Table 3 summarizes specific results from the models. Taken together, a greater reduction in both movement band power and burst durations were associated with improvement in bradykinesia.

Reductions in beta burst duration were associated with increased overlap of the VTM with the sensorimotor STN

There were inverse correlations between the reduction in both movement band power and burst duration and the degree of overlap of the volume of brain tissue modulated (VTM) with the entire STN as well as with the sensorimotor region of the STN (Fig. 4).

The top panel of Fig. 4 demonstrates that across the group, DBS electrode leads were placed in the sensorimotor STN (light blue). The middle panel shows a schematic of the STN (in yellow), sensorimotor STN (light blue), and the VTMs around the DBS lead at increasing DBS intensities from one individual. At 0% DBS the VTM was zero, as no tissue was modulated; at 25% V_{max} there was a small VTM within sensorimotor STN (highlighted in red); at 50% and 75% V_{max} the VTMs (blue and green, respectively) overlapped a greater volume of sensorimotor STN, and at 100% V_{max} the VTM overlapped almost the entire sensorimotor STN. Linear mixed effects regression models were used to assess the relationships between per cent change in either movement band power or burst duration and per cent change in VTM overlap with the entire STN or sensorimotor region of the STN (Fig. 4A and B). Activation of a greater percentage of the STN was associated with a greater reduction in movement band power ($\beta = -0.43$, $t = 6.93$, $P < 0.001$). However, activation of a greater percentage of specifically the sensorimotor portion of the STN was even more strongly related to reduction in movement band power ($\beta = -0.49$, $t = 9.08$, $P < 0.001$). Similarly, activation of a greater percentage of the STN was associated with greater reduction in movement band burst durations (Fig. 4A) ($\beta = -0.42$, $t = 7.92$, $P < 0.001$). However, again, activation of the sensorimotor STN was even more strongly related to reduction in movement band burst duration (Fig. 4B) ($\beta = -0.47$, $t = 10.35$, $P < 0.001$). Table 3 summarizes specific results from the models.

Degree of overlap of VTM with the sensorimotor STN and change in beta burst duration predict improvement in bradykinesia

A linear mixed effects regression model was used to test the interaction between the degree of overlap of the VTM with the sensorimotor STN and the change in movement band burst durations, on bradykinesia. There was a significant interaction between per cent VTM overlap with the sensorimotor STN and per cent change in movement band burst durations that was related to the per cent change in V_{rms} ($\beta = -0.18$, $t = 2.19$, $P < 0.05$). This association is visualized by the heat map in Fig. 5, which increased from dark blue, corresponding to small increases in V_{rms}, through green to yellow, corresponding to larger increases in V_{rms}. A greater percentage of VTM overlap with the sensorimotor STN and a greater reduction in movement band burst durations were associated with greater per cent increase in V_{rms}. A similar relationship was found between per cent change in V_{rms} and the interaction between the per cent VTM overlap with the sensorimotor STN and movement band power (Supplementary Fig. 2) ($\beta = -0.25$, $t = 2.72$, $P < 0.01$). Table 3 summarizes the results of these models.

Discussion

The results of this study demonstrate for the first time the relationship between a biomarker of Parkinson's disease, namely STN beta (movement band) power and burst durations, the location of the field of neuromodulation, and motor behaviour. This was achieved using synchronized subthalamic neural and kinematic recordings during a rWFE task from freely moving individuals with Parkinson's disease, who were implanted with a first generation sensing neurostimulator (Activa™ PC+S, Medtronic PLC) and who

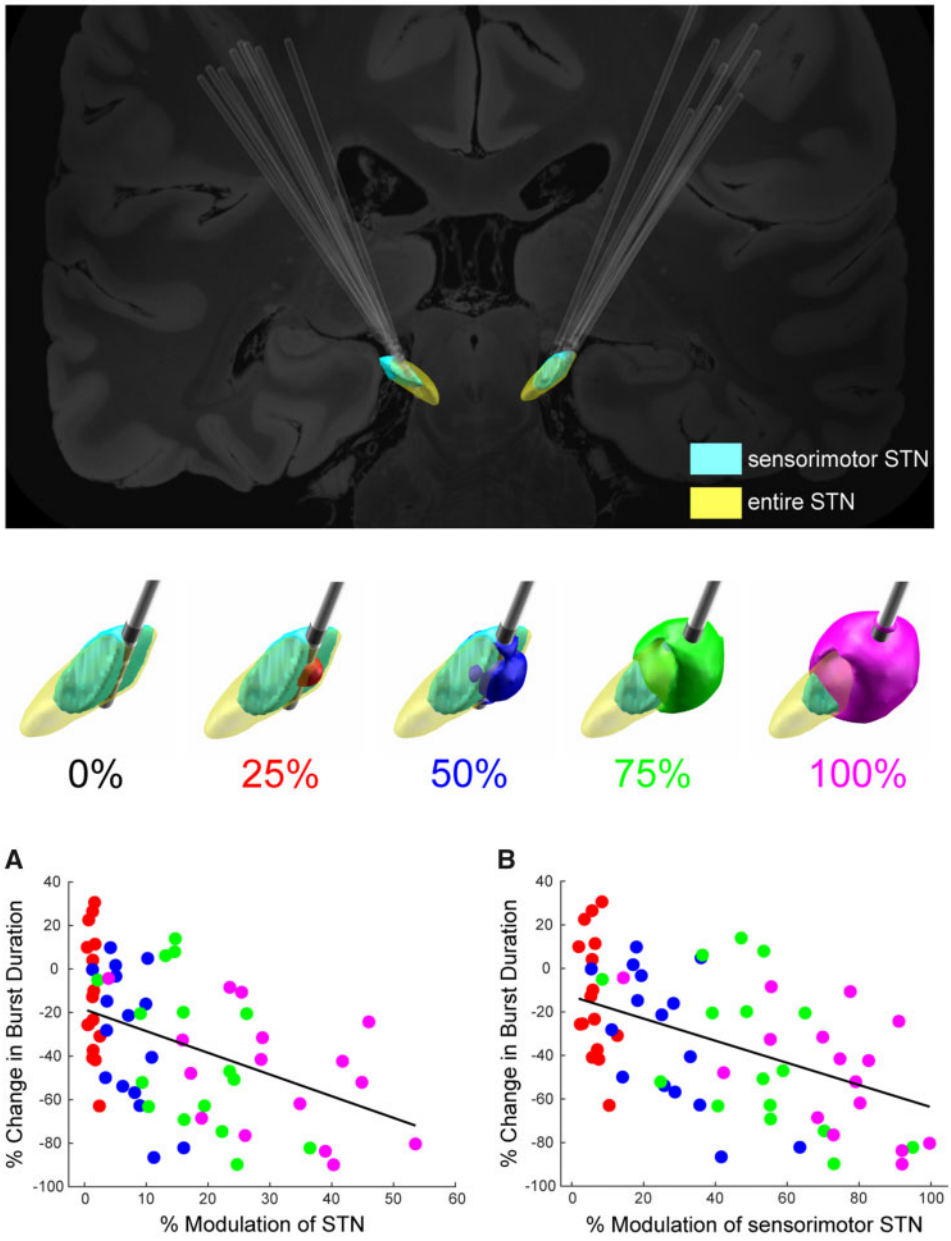

Figure 4 Change in beta power and burst duration was dependent on theoretical amount of tissue modulated in entire STN and sensorimotor STN. *Top*: DBS lead placement targeting sensorimotor STN (light blue) for all STN leads. *Middle*: Example of the VTM in one STN at 0%, 25% (red), 50% (blue), 75% (green), and 100% (magenta) V_{max} overlaid on the STN. The whole STN is depicted in yellow and the sensorimotor region is highlighted in light blue. *Bottom*: (**A**) Relationship between % change in movement band power and % modulation of the STN. (**B**) Relationship between the % change in movement band burst duration and % modulation of the sensorimotor portion of the STN. The % modulation of both the STN as a whole and of the sensorimotor region of the STN significantly predicted the change in burst duration, $P < 0.001$, with the stronger relationship observed for the sensorimotor portion of the STN.

had been receiving continuous high frequency DBS for a mean of 2.5 ± 0.6 years. Randomized incremental increases of STN DBS intensity during movement resulted in improvement in bradykinesia. This improvement was accompanied by a progressive reduction in movement band burst duration as well as in movement band power. The degree of reduction in movement band burst durations and power could be partially explained by the volume of tissue modulated in the STN, particularly in the sensorimotor region. Finally, the amount of tissue modulated in the sensorimotor STN, together with the degree of attenuation of both movement band burst duration and power, significantly predicted the improvement in bradykinesia. These results highlight the critical role that pathologically prolonged beta bursts and elevated beta power in the sensorimotor STN play in motor impairment in Parkinson's disease and point toward a direct

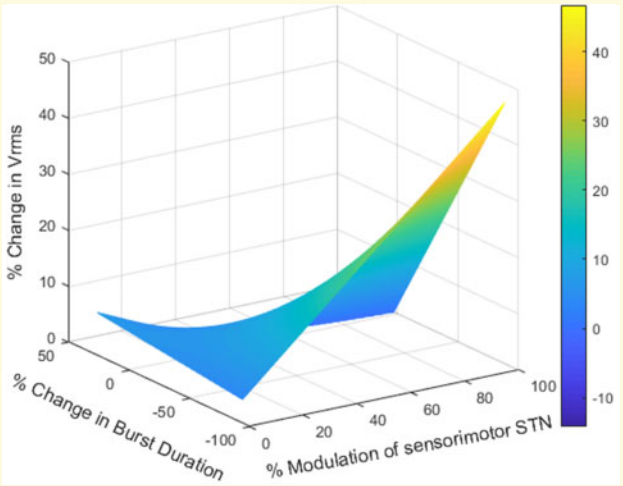

Figure 5 Change in movement band burst duration interacted with the amount of overlap of the VTM with the sensorimotor STN to predict the increase in V_{rms}. The heat map represents the 3D interaction among changes in movement band burst duration, % overlap of the VTM with the sensorimotor STN, and % increase in V_{rms}. Greater reduction in movement band burst duration and greater overlap of the VTM with the sensorimotor STN were associated with larger increases in the % change in V_{rms}, $P < 0.05$. Colour bar represents the % change in V_{rms}.

mechanism of STN DBS for improving behaviour, by attenuating pathological sensorimotor beta oscillations and restoring neural activity towards a more physiological state of lower power and shorter oscillations.

Lead location in and VTM of the sensorimotor STN relate to improvement of the beta oscillopathy and bradykinesia

In the current study, a greater VTM in the sensorimotor STN was associated with reduced movement band power, shortened movement band burst durations, and improved motor outcome. This is the first demonstration that placement of the DBS lead in, and modulation of the sensorimotor STN in individuals with Parkinson's disease was related to attenuation of movement band power and burst durations during movement that were associated with improvements in bradykinesia.

The efficacy of STN DBS depends on modulation of the sensorimotor network, which requires highly accurate placement of the DBS lead in small targets, such as the dorsolateral STN. Advances in neuroimaging have enabled visualization of DBS lead location in relation to sensorimotor circuitry. The Human Brain Connectome project has led to standardized anatomical atlases of brain circuitry (Sporns *et al.*, 2005; Horn *et al.*, 2014; Fornito and Bullmore, 2015; Horn and Blankenburg, 2016; Fox, 2018). DBS connectomic modelling has incorporated such anatomic atlases with higher resolution MRI and models of the VTMs at different DBS intensities to predict that the maximum therapeutic benefit of motor symptoms in Parkinson's disease is associated with modulation of the dorsolateral STN, which coincides with the functionally defined sensorimotor region (Herzog *et al.*, 2004; Butson and McIntyre, 2005; Butson *et al.*, 2011; Chaturvedi *et al.*, 2012; Caire *et al.*, 2013; Haynes and Haber, 2013; Akram *et al.*, 2017, Horn *et al.*, 2017*a*; Bot *et al.*, 2018; Ewert *et al.*, 2018; Dembek *et al.*, 2019). The beta oscillopathy also has a dorsoventral gradient of power in the STN, and recently it has been demonstrated that delivering neurostimulation to the DBS electrode closest to the site of maximal resting state beta power in the STN produced the best patient outcomes (Ince *et al.*, 2010; Yoshida *et al.*, 2010; Zaidel *et al.*, 2010; De Solages *et al.*, 2011; Connolly *et al.*, 2015; Milosevic *et al.*, 2020).

Here, we provide direct evidence for the interaction between lead placement, VTM of the STN sensorimotor region, the beta oscillopathy during movement, and the efficacy of STN DBS, which has only been theorized up to now. This evidence highlights the critical need to implement knowledge of lead location and/or VTMs into the standard DBS programming protocols to facilitate physician's choice of stimulation contact and amplitude.

DBS efficacy for improving bradykinesia was related to the modulation of the beta oscillopathy during movement

This is the first study to demonstrate that randomized incremental increases of STN DBS intensity during a repetitive movement task were accompanied by a dose-dependent (based on voltage) attenuation in movement band power and reduction in movement band burst duration, and furthermore that these reductions partially predicted dose-dependent improvements in bradykinesia. Rather than focusing on the low and high beta sub-bands to track this dose dependence, we focused on an STN-specific movement band, a 6 Hz band around the most elevated peak in the beta band during movement. The current electrophysiological results suggest that the effect of therapeutic DBS is to return the system closer to a physiological state. Increases in DBS intensity reduced beta power and shifted the spectral profile towards that resembling a 1/f curve as would be expected for non-oscillatory neural activity (He, 2014). Physiological beta burst durations in the sensorimotor network of the healthy non-human primate brain are $\leqslant$150 ms (Murthy and Fetz, 1992, 1996; Pfurtscheller *et al.*, 1996; Leventhal *et al.*, 2012; Feingold *et al.*, 2015). In the present study, the group mean movement band burst duration was 626 ± 554 ms off DBS, which decreased to 210 ± 5 ms during STN DBS at V_{max}. This supports the hypothesis that the effect of high frequency STN DBS during movement in individuals with Parkinson's disease is to progressively restore STN sensorimotor beta oscillations toward a more

physiological duration, and this was associated with restoring impaired movement toward a healthier state. These results solidify the role of beta oscillopathy as an effective biomarker of the hypokinetic state in Parkinson's disease. The advent of sensing neurostimulators means that this is a feasibly attainable clinical biomarker to use as a tool for tracking changes to therapy.

Implications for closed-loop DBS

The results of this study support the feasibility of using beta power or beta burst duration during movement as the control variable in neural closed-loop DBS. In contrast to conventional delivery of open-loop neurostimulation, closed-loop DBS is delivered in a feedback-responsive manner, controlled by dynamic control policy algorithms, based on neural or behavioural biomarkers of the disease state. Previous demonstrations of the inverse relationship between resting state beta band power and DBS intensity supported the dual threshold control policy algorithm we developed in the first demonstration of the feasibility of closed-loop STN DBS for bradykinesia and tremor in Parkinson's disease, using a fully implanted sensing neurostimulator (Whitmer *et al.*, 2012; Velisar *et al.*, 2019). We have also demonstrated efficacy of closed-loop DBS using the dual threshold control policy algorithm driven by movement state subject-specific sub-bands of beta power to improve bradykinesia (Afzal *et al.*, 2019). The current study highlights the fact that both movement band power and burst durations are relevant and useful control variables, as we have demonstrated that voltage-dependent reduction in both movement band power and mean movement band burst duration was correlated with improvement in bradykinesia. DBS intensity titrations can be used to identify the upper and lower beta band power and/or mean burst duration thresholds during movement to identify the patient-specific therapeutic range in which DBS intensity can change to modulate the biomarker of the hypokinetic state.

Previous studies used resting state beta band power as a biomarker for closed-loop DBS experiments and most were performed in the acute state using externalized leads and systems (Eusebio *et al.*, 2011; Little *et al.*, 2013, 2016*a*, *b*; Rosa *et al.*, 2015, 2017; Piña-Fuentes *et al.*, 2017, 2019; Arlotti *et al.*, 2018). There were concerns that beta power would be eliminated during movement, which would render beta control policy algorithms ineffective in improving behaviour (Johnson *et al.*, 2016; Little and Brown, 2020). However, this and previous studies have shown that STN LFP beta band power does not disappear and can still be tracked during ongoing movement in Parkinson's disease (Quinn *et al.*, 2015; Blumenfeld *et al.*, 2017; Steiner *et al.*, 2017; Syrkin-Nikolau *et al.*, 2017; Anidi *et al.*, 2018; Afzal *et al.*, 2019). Movement band burst durations mirrored movement band power in their association with impaired movement and inverse association with DBS intensity. This coupled with next generation sensing neurostimulator technology that allows for development of control policy algorithms based on beta burst duration (Summit^{TM} RC+S system, Medtronic PLC) supports movement band burst duration driven closed-loop DBS in freely moving Parkinson's disease subjects.

Limitations

One limitation of the current study is that the calculated VTMs are theoretical models of stimulation-induced modulation of STN. However, such models can provide an estimation of the interaction between different neurostimulation intensities and volumes of tissue modulated, depending on lead location. Another limitation is that the current study focused on the beta band due to its role in the pathophysiology in Parkinson's disease. There is evidence that the gamma band (Özkurt *et al.*, 2011; Swann *et al.*, 2016), beta-gamma phase amplitude coupling (De Hemptinne *et al.*, 2015; van Wijk *et al.*, 2016; Shreve *et al.*, 2017), and STN-cortical interactions (Shimamoto *et al.*, 2013) may also play a role in the mechanism of DBS. The Activa^{TM} PC+S was not able to record frequencies in the gamma range during stimulation. We also did not attempt to explore the interaction between beta power and burst duration on either V_{rms} or VTMs due to the high correlation between the two metrics. Finally, the overall sample size was similar to previous studies but still limited by the number of neurostimulators allocated to centres involved in the Activa^{TM} PC+S project.

Conclusion

The results of the current study revealed heretofore theorized mechanisms of STN DBS by elucidating the interaction between physiology (beta oscillations), anatomy (lead location), and behaviour (kinematics), through the use of synchronized neural and kinematic recordings during movement in chronically implanted individuals with Parkinson's disease. Specifically, the current study demonstrated that the improvement of bradykinesia during STN DBS depended on the reduction of beta power and beta burst durations during movement, and the degree of modulation of the sensorimotor region of the STN. In addition to the mechanistic insights for STN DBS in Parkinson's disease, these results highlight the feasibility of using beta power and burst durations during movement for closed-loop STN DBS, as these features are still measurable during movement, and during high frequency STN DBS, and their modulation was related to improvement in bradykinesia in a dose-dependent manner through DBS leads accurately placed in sensorimotor STN.

Acknowledgements

We would like to thank the members of the Human Motor Control and Neuromodulation laboratory, Dr Jaimie

Henderson, and, most importantly, the participants who dedicated their time to this study.

Funding

This work was supported in part by the following: NINDS UH3NS107709, NINDS R21 NS096398-02, Michael J. Fox Foundation (9605), Parkinson's Foundation - Postdoctoral Fellowship PF-FBS-2024, Robert and Ruth Halperin Foundation, John A. Blume Foundation, John E Cahill Family Foundation, and Medtronic PLC who provided the devices used in this study but no additional financial support.

Competing interests

H.M.B-S. serves on a clinical advisory board for Medtronic PLC.

Supplementary material

Supplementary material is available at *Brain* online.

References

Afzal MF, Velisar A, Anidi C, Neuville R, Prabhakar V, Bronte-Stewart HM. Abstract #96: subthalamic neural closed-loop deep brain stimulation for bradykinesia in Parkinson's disease. Brain Stimul 2019; 12: E33.

Akram H, Georgiev D, Mahlknecht P, Hyam J, Foltynie T, Limousin P, et al. Subthalamic deep brain stimulation sweet spots and hyperdirect cortical connectivity in Parkinson's disease. Neuroimage 2017; 158: 332–45.

Anderson RW, Kehnemouyi YM, Neuville RS, Wilkins KB, Anidi CM, Petrucci MN, et al. A novel method for calculating beta band burst durations in Parkinson's disease using a physiological baseline. J Neurosci Methods 2020; 343: 108811.doi: 10.1016/j.jneumeth.2020.108811.

Anidi C, O'Day JJ, Anderson RW, Afzal MF, Syrkin-Nikolau J, Velisar A, et al. Neuromodulation targets pathological not physiological beta bursts during gait in Parkinson's disease. Neurobiol Dis 2018; 120: 107–17.

Arlotti M, Marceglia S, Foffani G, Volkmann J, Lozano AM, Moro E, et al. Eight-hours adaptive deep brain stimulation in patients with Parkinson disease. Neurology 2018; 90: e971–6.

Avants BB, Tustison NJ, Song G, Cook PA, Klein A, Gee JC. A reproducible evaluation of ANTs similarity metric performance in brain image registration. Neuroimage 2011; 54: 2033–44.

Blumenfeld Z, Koop MM, Prieto TE, Shreve LA, Velisar A, Quinn EJ, et al. Sixty-hertz stimulation improves bradykinesia and amplifies subthalamic low-frequency oscillations. Mov Disord 2017; 32: 80–8.

Bot M, Schuurman PR, Odekerken VJJ, Verhagen R, Contarino FM, De Bie RMA, et al. Deep brain stimulation for Parkinson's disease: defining the optimal location within the subthalamic nucleus. J Neurol Neurosurg Psychiatry 2018; 89: 493–8.

Bronte-Stewart H, Barberini C, Koop MM, Hill BC, Henderson JM, Wingeier B. The STN beta-band profile in Parkinson's disease is stationary and shows prolonged attenuation after deep brain stimulation. Exp Neurol 2009; 215: 20–8.

Brontë-Stewart H, Louie S, Batya S, Henderson JM. Clinical motor outcome of bilateral subthalamic nucleus deep-brain stimulation for Parkinson's disease using image-guided frameless stereotaxy. Neurosurgery 2010; 67: 1088–93.

Brown P, Oliviero A, Mazzone P, Insola A, Tonali P, Di Lazzaro V. Dopamine dependency of oscillations between subthalamic nucleus and pallidum in Parkinson's disease. J Neurosci 2001; 21: 1033–8.

Butson CR, Cooper SE, Henderson JM, Wolgamuth B, McIntyre CC. Probabilistic analysis of activation volumes generated during deep brain stimulation. Neuroimage 2011; 54: 2096–104.

Butson CR, McIntyre CC. Tissue and electrode capacitance reduce neural activation volumes during deep brain stimulation. Clin Neurophysiol 2005; 116: 2490–500.

Caire F, Ranoux D, Guehl D, Burbaud P, Cuny E. A systematic review of studies on anatomical position of electrode contacts used for chronic subthalamic stimulation in Parkinson's disease. Acta Neurochir 2013; 155: 1647–54.

Cassidy M, Mazzone P, Oliviero A, Insola A, Tonali P, Di Lazzaro V, et al. Movement-related changes in synchronization in the human basal ganglia. Brain 2002; 125: 1235–46.

Chaturvedi A, Foutz TJ, McIntyre CC. Current steering to activate targeted neural pathways during deep brain stimulation of the subthalamic region. Brain Stimul 2012; 5: 369–77.

Connolly AT, Muralidharan A, Hendrix C, Johnson L, Gupta R, Stanslaski S, et al. Local field potential recordings in a non-human primate model of Parkinsons disease using the Activa PC + S neurostimulator. J Neural Eng 2015; 12: 066012.

Deffains M, Iskhakova L, Katabi S, Israel Z, Bergman H. Longer β oscillatory episodes reliably identify pathological subthalamic activity in Parkinsonism. Mov Disord 2018; 33: 1609–18.

Dembek TA, Roediger J, Horn A, Reker P, Oehrn C, Dafsari HS, et al. Probabilistic sweet spots predict motor outcome for deep brain stimulation in Parkinson disease. Ann Neurol 2019; 86: 527–38.

De Hemptinne C, Swann NC, Ostrem JL, Ryapolova-Webb ES, San Luciano M, Galifianakis NB, et al. Therapeutic deep brain stimulation reduces cortical phase-amplitude coupling in Parkinson's disease. Nat Neurosci 2015; 18: 779–86.

De Solages C, Hill BC, Yu H, Henderson JM, Bronte-Stewart H. Maximal subthalamic beta hypersynchrony of the local field potential in Parkinson's disease is located in the central region of the nucleus. J Neurol Neurosurg Psychiatry 2011; 82: 1387–9.

Eusebio A, Thevathasan W, Doyle Gaynor L, Pogosyan A, Bye E, Foltynie T, et al. Deep brain stimulation can suppress pathological synchronisation in Parkinsonian patients. J Neurol Neurosurg Psychiatry 2011; 82: 569–73.

Ewert S, Plettig P, Li N, Chakravarty MM, Collins DL, Herrington TM, et al. Toward defining deep brain stimulation targets in MNI space: a subcortical atlas based on multimodal MRI, histology and structural connectivity. Neuroimage 2018; 170: 271–82.

Feingold J, Gibson DJ, Depasquale B, Graybiel AM. Bursts of beta oscillation differentiate postperformance activity in the striatum and motor cortex of monkeys performing movement tasks. Proc Natl Acad Sci USA 2015; 112: 13687–92.

Fornito A, Bullmore ET. Connectomics: a new paradigm for understanding brain disease. Eur Neuropsychopharmacol 2015; 25: 733–48.

Fox MD. Mapping symptoms to brain networks with the human connectome. N Engl J Med 2018; 379: 2237–45.

Giannicola G, Marceglia S, Rossi L, Mrakic-Sposta S, Rampini P, Tamma F, et al. The effects of levodopa and ongoing deep brain stimulation on subthalamic beta oscillations in Parkinson's disease. Exp Neurol 2010; 226: 120–7.

Haynes WIA, Haber SN. The organization of prefrontal-subthalamic inputs in primates provides an anatomical substrate for both functional specificity and integration: implications for basal ganglia models and deep brain stimulation. J Neurosci 2013; 33: 4804–14.

He BJ. Scale-free brain activity: past, present, and future. Trends Cogn Sci 2014; 18: 480–7.

Hell F, Plate A, Mehrkens JH, Bötzel K. Subthalamic oscillatory activity and connectivity during gait in Parkinson's disease. NeuroImage Clin 2018; 19: 396–405.

Herzog J, Fietzek U, Hamel W, Morsnowski A, Steigerwald F, Schrader B, et al. Most effective stimulation site in subthalamic deep brain stimulation for Parkinson's disease. Mov Disord 2004; 19: 1050–4.

Horn A, Blankenburg F. Toward a standardized structural-functional group connectome in MNI space. Neuroimage 2016; 124: 310–22.

Horn A, Kühn AA. Lead-DBS: a toolbox for deep brain stimulation electrode localizations and visualizations. Neuroimage 2015; 107: 127–35.

Horn A, Li N, Dembek TA, Kappel A, Boulay C, Ewert S, et al. Lead-DBS v2: towards a comprehensive pipeline for deep brain stimulation imaging. Neuroimage 2019; 184: 293–316.

Horn A, Neumann WJ, Degen K, Schneider GH, Kühn AA. Toward an electrophysiological "Sweet spot" for deep brain stimulation in the subthalamic nucleus. Hum Brain Mapp 2017a; 38: 3377–90.

Horn A, Ostwald D, Reisert M, Blankenburg F. The structural-functional connectome and the default mode network of the human brain. Neuroimage 2014; 102: 142–51.

Horn A, Reich M, Vorwerk J, Li N, Wenzel G, Fang Q, et al. Connectivity predicts deep brain stimulation outcome in Parkinson disease. Ann Neurol 2017b; 82: 67–78.

Husch A, V. Petersen M, Gemmar P, Goncalves J, Hertel F. PaCER—a fully automated method for electrode trajectory and contact reconstruction in deep brain stimulation. NeuroImage Clin 2018; 17: 80–9.

Ince NF, Gupte A, Wichmann T, Ashe J, Henry T, Bebler M, et al. Selection of optimal programming contacts based on local field potential recordings from subthalamic nucleus in patients with Parkinson's disease. Neurosurgery 2010; 67: 390–7.

Johnson LA, Nebeck SD, Muralidharan A, Johnson MD, Baker KB, Vitek JL. Closed-loop deep brain stimulation effects on Parkinsonian motor symptoms in a non-human primate—is beta enough? Brain Stimul 2016; 9: 892–6.

Koop MM, Andrzejewski A, Hill BC, Heit G, Bronte-Stewart HM. Improvement in a quantitative measure of bradykinesia after microelectrode recording in patients with Parkinson's disease during deep brain stimulation surgery. Mov Disord 2006; 21: 673–8.

Koop MM, Shivitz N, Brontë-Stewart H. Quantitative measures of fine motor, limb, and postural bradykinesia in very stage, untreated Parkinson's disease. Mov Disord 2008; 23: 1262–8.

Kühn AA, Kempf F, Brücke C, Doyle LG, Martinez-Torres I, Pogosyan A, et al. High-frequency stimulation of the subthalamic nucleus suppresses oscillatory β activity in patients with Parkinson's disease in parallel with improvement in motor performance. J Neurosci 2008; 28: 6165–73.

Leventhal DK, Gage GJ, Schmidt R, Pettibone JR, Case AC, Berke JD. Basal ganglia beta oscillations accompany cue utilization. Neuron 2012; 73: 523–36.

Levy R, Ashby P, Hutchison WD, Lang AE, Lozano AM, Dostrovsky JO. Dependence of subthalamic nucleus oscillations on movement and dopamine in Parkinson's disease. Brain 2002; 125: 1196–209.

Little S, Beudel M, Zrinzo L, Foltynie T, Limousin P, Hariz M, et al. Bilateral adaptive deep brain stimulation is effective in Parkinson's disease. J Neurol Neurosurg Psychiatry 2016a; 87: 717–21.

Little S, Brown P. Debugging adaptive deep brain stimulation for Parkinson's disease. Mov Disord 2020; 35: 555–61.

Little S, Pogosyan A, Neal S, Zavala B, Zrinzo L, Hariz M, et al. Adaptive deep brain stimulation in advanced Parkinson disease. Ann Neurol 2013; 74: 449–57.

Little S, Tripoliti E, Beudel M, Pogosyan A, Cagnan H, Herz D, et al. Adaptive deep brain stimulation for Parkinson's disease demonstrates reduced speech side effects compared to conventional stimulation in the acute setting. J Neurol Neurosurg Psychiatry 2016b; 87: 1388–9.

Louie S, Koop MM, Frenklach A, Bronte-Stewart H. Quantitative lateralized measures of bradykinesia at different stages of Parkinson's disease: the role of the less affected side. Mov Disord 2009; 24: 1991–7.

Milosevic L, Scherer M, Cebi I, Guggenberger R, Machetanz K, Naros G, et al. Online mapping with the deep brain stimulation lead: a novel targeting tool in Parkinson's disease. Mov Disord 2020; 35: 1574–86.

Murthy VN, Fetz EE. Coherent 25- To 35-Hz oscillations in the sensorimotor cortex of awake behaving monkeys. Proc Natl Acad Sci USA 1992; 89: 5670–74.

Murthy VN, Fetz EE. Oscillatory activity in sensorimotor cortex of awake monkeys: synchronization of local field potentials and relation to behavior. J Neurophysiol 1996; 76: 3949–67.

Özkurt TE, Butz M, Homburger M, Elben S, Vesper J, Wojtecki L, et al. High frequency oscillations in the subthalamic nucleus: a neurophysiological marker of the motor state in Parkinson's disease. Exp Neurol 2011; 229: 324–31.

Pfurtscheller G, Stancák A, Neuper C. Post-movement beta synchronization. A correlate of an idling motor area? Electroencephalogr Clin Neurophysiol 1996; 98: 281–93.

Piña-Fuentes D, Little S, Oterdoom M, Neal S, Pogosyan A, Tijssen MAJ, et al. Adaptive DBS in a Parkinson's patient with chronically implanted DBS: a proof of principle. Mov Disord 2017; 32: 1253–54.

Piña-Fuentes D, van Zijl JC, van Dijk JMC, Little S, Tinkhauser G, Oterdoom DLM, et al. The characteristics of pallidal low-frequency and beta bursts could help implementing adaptive brain stimulation in the Parkinsonian and dystonic internal globus pallidus. Neurobiol Dis 2019; 121: 47–57.

Priori A, Foffani G, Pesenti A, Tamma F, Bianchi AM, Pellegrini M, et al. Rhythm-specific pharmacological modulation of subthalamic activity in Parkinson's disease. Exp Neurol 2004; 189: 369–79.

Quinn EJ, Blumenfeld Z, Velisar A, Koop MM, Shreve LA, Trager MH, et al. Beta oscillations in freely moving Parkinson's subjects are attenuated during deep brain stimulation. Mov Disord 2015; 30: 1750–8.

Ray NJ, Jenkinson N, Wang S, Holland P, Brittain JS, Joint C, et al. Local field potential beta activity in the subthalamic nucleus of patients with Parkinson's disease is associated with improvements in bradykinesia after dopamine and deep brain stimulation. Exp Neurol 2008; 213: 108–13.

Rosa M, Arlotti M, Ardolino G, Cogiamanian F, Marceglia S, D, Fonzo, A, et al. Adaptive deep brain stimulation in a freely moving parkinsonian patient. Mov Disord 2015; 30: 1003–5.

Rosa M, Arlotti M, Marceglia S, Cogiamanian F, Ardolino G, Fonzo AD, et al. Adaptive deep brain stimulation controls levodopa-induced side effects in Parkinsonian patients. Mov Disord 2017; 32: 628–9.

Shimamoto SA, Ryapolova-Webb ES, Ostrem JL, Galifianakis NB, Miller KJ, Starr PA. Subthalamic nucleus neurons are synchronized to primary motor cortex local field potentials in Parkinson's disease. J Neurosci 2013; 33: 7220–33.

Shreve LA, Velisar A, Malekmohammadi M, Koop MM, Trager M, Quinn EJ, et al. Subthalamic oscillations and phase amplitude coupling are greater in the more affected hemisphere in Parkinson's disease. Clin Neurophysiol 2017; 128: 128–37.

Sporns O, Tononi G, Kötter R. The human connectome: a structural description of the human brain. PLoS Comput Biol 2005; 1: e42.

Steiner LA, Neumann WJ, Staub-Bartelt F, Herz DM, Tan H, Pogosyan A, et al. Subthalamic beta dynamics mirror Parkinsonian bradykinesia months after neurostimulator implantation. Mov Disord 2017; 32: 1183–90.

Swann NC, De Hemptinne C, Miocinovic S, Qasim S, Wang SS, Ziman N, et al. Gamma oscillations in the hyperkinetic state detected with chronic human brain recordings in Parkinson's disease. J Neurosci 2016; 36: 6445–58.

Syrkin-Nikolau J, Koop MM, Prieto T, Anidi C, Afzal MF, Velisar A, et al. Subthalamic neural entropy is a feature of freezing of gait in

freely moving people with Parkinson's disease. Neurobiol Dis 2017; 108: 288–97.

Tinkhauser G, Pogosyan A, Little S, Beudel M, Herz DM, Tan H, et al. The modulatory effect of adaptive deep brain stimulation on beta bursts in Parkinson's disease. Brain 2017; 140: 1053–67.

Trager MH, Koop MM, Velisar A, Blumenfeld Z, Nikolau JS, Quinn EJ, et al. Subthalamic beta oscillations are attenuated after withdrawal of chronic high frequency neurostimulation in Parkinson's disease. Neurobiol Dis 2016; 96: 22–30.

van Wijk BCM, Beudel M, Jha A, Oswal A, Foltynie T, Hariz MI, et al. Subthalamic nucleus phase-amplitude coupling correlates with motor impairment in Parkinson's disease. Clin Neurophysiol 2016; 127: 2010–9.

Vanegas-Arroyave N, Lauro PM, Huang L, Hallett M, Horovitz SG, Zaghloul KA, et al. Tractography patterns of subthalamic nucleus deep brain stimulation. Brain 2016; 139: 1200–10.

Velisar A, Syrkin-Nikolau J, Blumenfeld Z, Trager MH, Afzal MF, Prabhakar V, et al. Dual threshold neural closed loop deep brain stimulation in Parkinson disease patients. Brain Stimul 2019; 12: 868–76.

Whitmer D, de Solages C, Hill B, Yu H, Henderson JM, Bronte-Stewart H. High frequency deep brain stimulation attenuates subthalamic and cortical rhythms in Parkinson's disease. Front Hum Neurosci 2012; 6: 155.

Wingeier B, Tcheng T, Koop MM, Hill BC, Heit G, Bronte-Stewart HM. Intra-operative STN DBS attenuates the prominent beta rhythm in the STN in Parkinson's disease. Exp Neurol 2006; 197: 244–51.

Yoshida F, Martinez-Torres I, Pogosyan A, Holl E, Petersen E, Chen CC, et al. Value of subthalamic nucleus local field potentials recordings in predicting stimulation parameters for deep brain stimulation in Parkinson's disease. J Neurol Neurosurg Psychiatry 2010; 81: 885–9.

Zaidel A, Spivak A, Grieb B, Bergman H, Israel Z. Subthalamic span of β oscillations predicts deep brain stimulation efficacy for patients with Parkinson's disease. Brain 2010; 133: 2007–21.